PROCEEDINGS OF SPIE

SPIEDigitalLibrary.org/conference-proceedings-of-spie

High performance GaN/AlGaN ultraviolet avalanche photodiode detector technologies

Ashok K. Sood, John W. Zeller, Parminder Ghuman, Sachidananda Babu, Russell D. Dupuis

Ashok K. Sood, John W. Zeller, Parminder Ghuman, Sachidananda Babu, Russell D. Dupuis, "High performance GaN/AlGaN ultraviolet avalanche photodiode detector technologies," Proc. SPIE 10980, Image Sensing Technologies: Materials, Devices, Systems, and Applications VI, 109800M (13 May 2019); doi: 10.1117/12.2521464

SPIE.

Event: SPIE Defense + Commercial Sensing, 2019, Baltimore, Maryland, United States

High Performance GaN/AlGaN Ultraviolet Avalanche Photodiode Detector Technologies

Ashok K. Sood and John W. Zeller

Magnolia Optical Technologies, Inc., 52-B Cummings Park, Suite 314, Woburn, MA, USA 01801

Parminder Ghuman and Sachidananda Babu

NASA Earth Science Technology Office, Greenbelt, MD, USA 20771

Russell D. Dupuis

School of Electrical and Computer Engineering, Georgia Institute of Technology, Atlanta, GA, USA 30332

ABSTRACT

Detection of ultraviolet (UV) bands provides distinct advantages for NASA, defense, and commercial applications, including increased spatial resolution, small pixel sizes, and large format arrays. $Al_xGa_{1-x}N$ semiconductor alloys have attracted great interest for detection in the UV spectral region because of their potential for high optical gain, high sensitivity, and low dark current performance in ultraviolet avalanche photodiodes (UV-APDs). We are developing GaN/AlGaN UV-APDs that demonstrate consistent and reliable UV-APD performance and operation. For these UV detectors we have measured gains of above 5×10^6 and high quantum efficiencies at ~350 nm enabled by a strong avalanche multiplication process. These UV-APDs are fabricated through high quality metal organic chemical vapor deposition (MOCVD) growth on lattice-matched, low dislocation density GaN substrates with optimized GaN/AlGaN UV-APD material growth and doping parameters. The high performance, variable-area GaN/AlGaN UV-APD detectors and arrays can be customized to a wide variety of sizes including large-area formats to enable sensing and high-resolution detection over UV bands of interest.

Keywords: Avalanche photodiodes, ultraviolet, GaN, AlGaN, MOCVD, high gain, thin films

1. INTRODUCTION

For many space and defense applications, spectral information beyond that which can be provided by conventional visible sensors are desired especially where covertness is a requirement. Detection of shorter wavelengths over the UV spectrum provides greater spatial resolutions, which allows for various pixel sizes and larger formats [1-3]. UV sensing applications include chemical and biological detection of surface residues and bio-aerosol agents, machine vision, and space research for NASA and defense applications [4].

Avalanche photodiodes (APDs) based on AlGaN semiconductor alloys offer advantages of high optical gains, high sensitivity, low dark currents, and chemical and thermal stability for many demanding applications [4]. Development of arrays of APD pixels as small as 4 μm is achievable with this material technology [1]. Since the operating wavelength range of $Al_xGa_{1-x}N$ APDs is adjustable by controlling the Al concentration in the material, these devices can be designed to detect photons over large portions of the UV spectrum.

Growth of AlGaN material for high gain ultraviolet avalanche photodiode (UV-APD) arrays has traditionally been restricted to the use of lattice-mismatched substrates such as SiC and sapphire due to the lack of availability of native III-N substrates [5]. However, the lattice mismatch and differences in the thermal expansion coefficients between such foreign substrates can lead to strain-induced defects, resulting in high leakage current and premature microplasma breakdown prior to reaching avalanche breakdown [6]. To improve the growth process, low dislocation density *n*-type GaN substrates are employed to successfully improve the crystalline and structural quality of the epitaxial layers.

Image Sensing Technologies: Materials, Devices, Systems, and Applications VI, edited by Nibir K. Dhar, Achyut K. Dutta, Sachidananda R. Babu, Proc. of SPIE Vol. 10980, 109800M · © 2019 SPIE
CCC code: 0277-786X/19/$18 · doi: 10.1117/12.2521464

To advance the technology for UV detection, Magnolia has collaborated with the Georgia Institute of Technology to develop GaN/AlGaN ultraviolet avalanche photodiodes (UV-APDs) and UV-APD arrays on lattice-matched GaN substrates for high-sensitivity UV sensing and imaging. Metalorganic chemical vapor deposition (MOCVD) is being utilized for epitaxial growth of the GaN/AlGaN UV-APD detectors and arrays. These high-performance detectors and arrays providing improved frontside-illuminated performance are being developed to enable high resolution imaging at the ~355 nm wavelength of interest.

2. FABRICATION OF GAN/ALGAN UV-APD DEVICES

2.1 UV-APD design and fabrication process

GaN *p-i-p-i-n* separate absorption and multiplication (SAM) UV-APDs with large detection areas grown by MOCVD have been fabricated on bulk GaN substrates having low defect densities. The fabricated UV-APDs with *p*-type $Al_{0.05}Ga_{0.95}N$ layers were found to exhibit narrower responsivity ranges over a shorter wavelength region relative to UV-APDs with *p*-type GaN layers, confirming that the *p*-type $Al_{0.05}Ga_{0.95}N$ layer functions as a window layer. This results in reduction of UV light absorption in the *p*-type contact layer, thus allowing higher absorption to occur in the absorption layer. For further enhancement of the responsivity and external quantum efficiency (EQE) of the front-illuminated UV-APDs, a higher-Al-composition *p*-type $Al_xGa_{1-x}N$ layer or thicker absorption layer can be used.

Fabrication of the GaN/AlGaN *p-i-p-i-n* UV-APDs with SAM regions has been carried out utilizing MOCVD growth. Figure 1(a) shows the growth chamber of the AIXTRON MOCVD growth reactor at Georgia Tech, which provides uniformity control for growth of high quality GaN and AlGaN material with doping for UV-APD applications [7]. The substrates used are composed of *n*-type Si-doped bulk GaN having threading dislocation densities lower than 5×10^4 cm^{-2}. For the frontside-illuminated electron-initiated multiplication process, a *p*-type $Al_{0.05}Ga_{0.95}N$:Mg layer was introduced as a window layer instead of a *p*-GaN:Mg layer to reduce the UV-light absorption in the *p*-type contact layer.

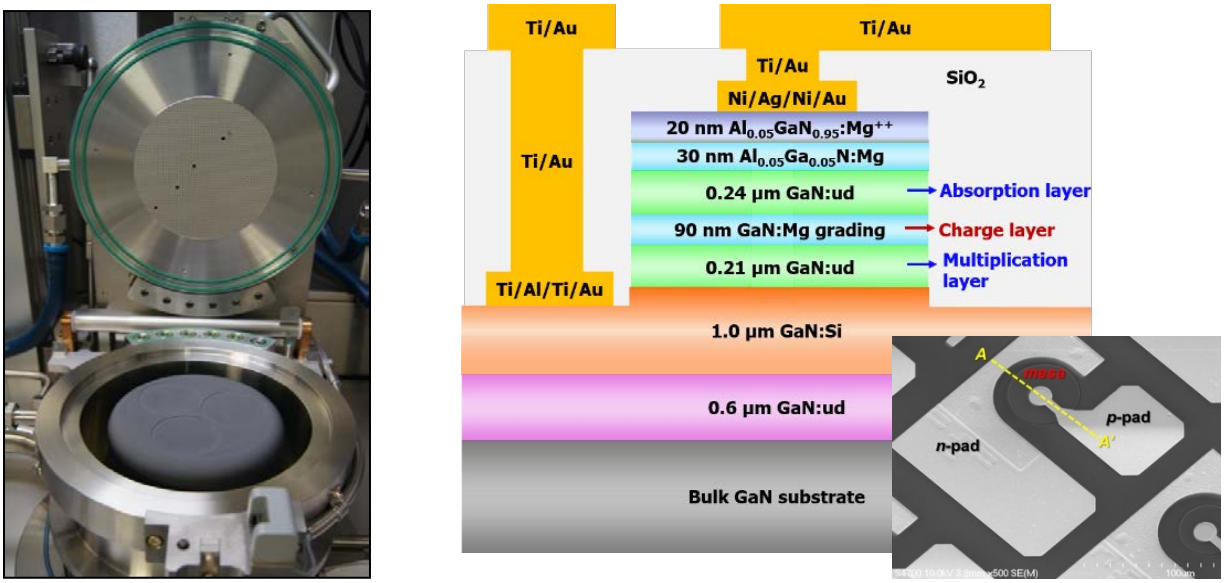

Figure 1: (a) III-nitride MOCVD growth chamber with close-coupled showerhead, part of high-temperature MOCVD system at Georgia Tech [7]. (b) Schematic cross-sectional structure of a top-illuminated GaN/AlGaN *p-i-p-i-n* UV-APD with AlGaN:Mg *p*-type window grown on a bulk GaN substrate; inset shows SEM image showing top view of APD physical layout [6].

These GaN/AlGaN UV-APDs have been fabricated with mesa sizes ranging from 2,000 μm^2 to 10,000 μm^2 by low damage inductively coupled plasma reactive-ion etching (ICP-RIE). Figure 1(b) shows the schematic cross-sectional structure for the fabricated GaN/AlGaN *p-i-p-i-n* UV-APDs, where a top-view scanning electron microscopy (SEM) image of the APD physical layout showing the metal contact pads and circular mesa is given in the inset [6]. Ti/Al/Ti/Au and Ni/Ag/Ni/Au metal stacks were evaporated and annealed on the *n*-type and *p*-type contact layers, respectively. To suppress mesa sidewall

leakage current and prevent premature breakdown under high reverse bias, a SiO_2 passivation layer was deposited using plasma-enhanced chemical vapor deposition (PECVD) with accessing via holes opened by subsequent ICP-RIE. Finally, thick Ti/Au metal stacks were evaporated for metal interconnects and bonding pads.

2.2 Modeling of UV-APD electrical behavior

These UV-APDs with reduced breakdown voltage offer reduced microplasma formation, lower DC bias for single-photon detection, and lower power consumption compared to conventional APD designs. Beyond the breakdown voltage, a sharp increase of the dark current density is observed. This steep breakdown voltage (V_{BR}) implies that the avalanche multiplication process involving impact ionization in the multiplication region occurs predominantly under high electric fields, enabling higher photon detection efficiencies. No microplasma breakdown or premature junction breakdown from sidewalls were observed at reverse bias voltages past the onset of the breakdown voltage based on multiple I-V scans.

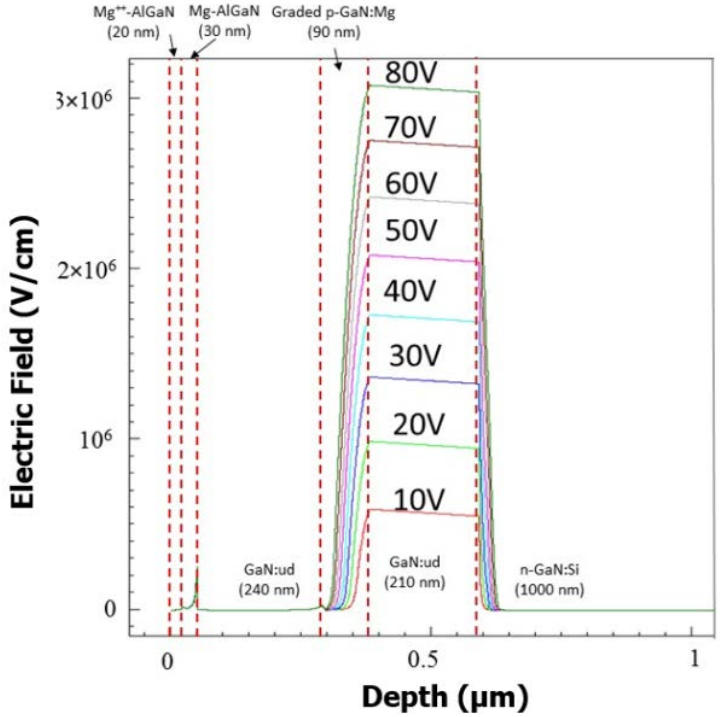

Figure 2: Voltage-dependent electric field distribution of a GaN/AlGaN UV-APDs.

The calculated electric field distributions of the UV-APDs at various reverse biases are shown in Figure 2. The simulation was conducted using Sentaurus TCAD software with parameters relevant to the simulation. The charge layer serves as a field-termination layer, which prevents further extension of the electric field through the lightly *p*-type doped absorption layer caused by the slow turn-off transient of the magnesium dopant source. In addition, the extension of the depletion region from the absorption layer is impeded by the decreased electric field in the graded *p*-type charge layer, which further increases the electric field in the depleted multiplication region. As demonstrated by modeling of the device, the maximum electric field profile in the multiplication region exceeds 3 MV/cm at a V_{BR} of 80 V, a typical critical breakdown electric field strength for GaN/AlGaN UV-APDs.

3. GAN/ALGAN UV-APD MATERIAL CHARACTERIZATION

In order to examine the surface morphology and crystal quality of the epitaxial layer structure, characterization techniques including atomic-force microscopy (AFM), Nomarski optical microscopy, X-ray diffraction (XRD), and secondary ion mass spectrometry (SIMS) have been utilized. The AlN mole fractions in the $Al_xGa_{1-x}N$ epitaxial layers were determined by XRD measurements. In addition, Hall-effect measurements at 300 K were used to measure the electrical properties of *p*-$Al_{0.05}Ga_{0.95}N$:Mg and *n*-GaN:Si layers.

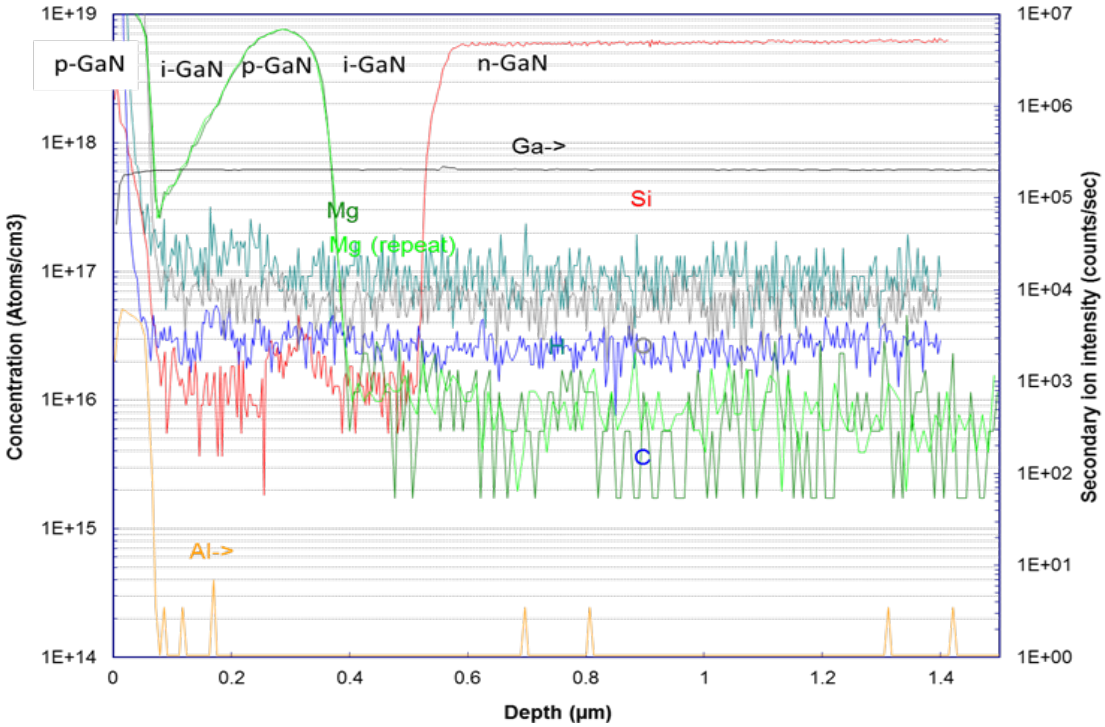

Figure 3: SIMS profile of a GaN/AlGaN UV-APD with AlGaN: Mg *p*-type window grown on bulk GaN substrate.

SIMS was employed to investigate and confirm the actual doping profile and thickness of each layer, as shown plotted in Figure 3. The free-hole concentration of *p*-$Al_{0.05}Ga_{0.95}N$:Mg was estimated to be $p \sim 4.9\times10^{17}$ cm^{-3} with a mobility of ~7.4 $cm^2/V\cdot s$, resulting in a resistivity of ~1.7 Ω-cm. The free-electron concentration of the *n*-GaN:Si layer was estimated to be $n \sim 5.0\times10^{18}$ cm^{-3} with a mobility of 237 $cm^2/V\cdot s$ at room temperature.

Atomic-force microscopy (AFM) was used to characterize the surface properties of the UV-APD arrays. Figure 4 shows the microscopic surface morphology of a UV-APD grown on a bulk GaN substrate. The APD wafers revealed smooth surfaces and well-developed step-flow morphologies without any visible nanopits and dislocation-induced surface features with root mean square surface roughness values of 0.113 and 0.137 for 1×1 μm^2 and 5×5 μm^2 scans, respectively. These results indicate significant improvement in the crystalline quality of the UV-APDs grown on the bulk GaN substrates.

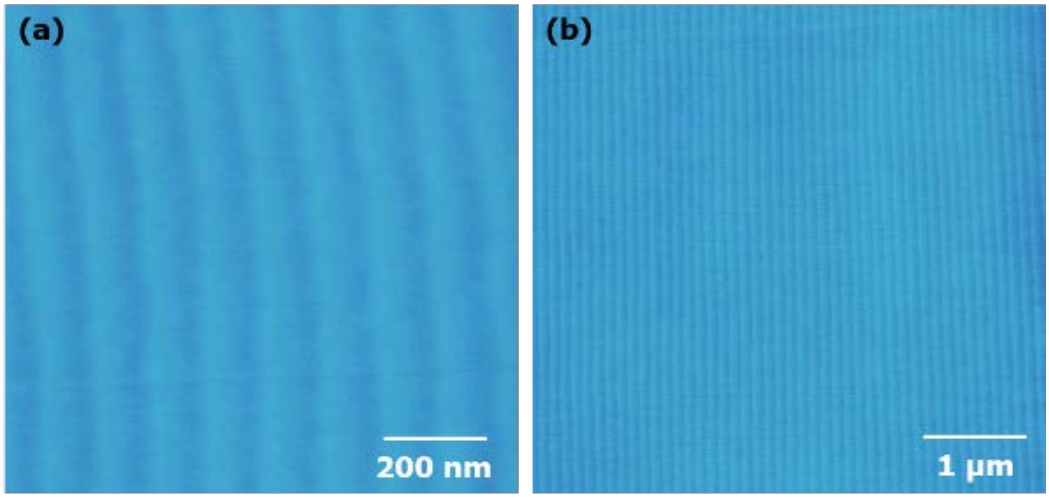

Figure 4: AFM microscopic surface morphology of GaN/AlGaN UV-APD grown on a bulk GaN substrate: (a) with 1×1 μm^2 scan; and (b) with 5×5 μm^2 scan with *z*-height scale of 10 nm.

4. GAN/ALGAN UV-APD ELECTRO-OPTICAL PERFORMANCE

4.1 I-V and gain characteristics

The current-voltage (I-V) and gain characteristics of the GaN/AlGaN UV-APDs were measured using a Keithley Model 4200 Semiconductor characterization system under dark conditions and UV illumination with peak wavelength of 340 nm. Figure 5 shows the dark-current density, photocurrent density, and the calculated avalanche gain for a UV-APD having 75×75 μm^2 mesa size (detection area of 5,625 μm^2). The avalanche gain was calculated as:

$$Gain = \frac{I_{photo} - I_{dark}}{I_{photo(unity)} - I_{dark(unity)}} \quad (1)$$

where I_{photo} is the reverse-biased photocurrent, I_{dark} the dark current, $I_{photo(unity)}$ represents the average low-bias photocurrent, and $I_{dark(unity)}$ the low-bias dark current.

Under dark conditions, the UV-APD with separate absorption and multiplication regions exhibited a low leakage current of ~5.6×10^{-14} A, corresponding to a dark current density of below 1.0×10^{-9} A/cm^2 up to a reverse bias of 40 V. The low dark current density shows that the concentration of defects in this structure is quite low. The dark current then monotonically increased until reaching the onset point of breakdown voltage. Under UV illumination at 340 nm, this UV-APD showed a photocurrent density of 5.6×10^{-6} A/cm^2, which remained relatively constant and around four orders of magnitude higher that the dark current density up to a reverse bias of ~40 V. As the magnitude of the reverse bias increased further, the behavior of the photocurrent density exhibited a similar trend to that of the dark current density.

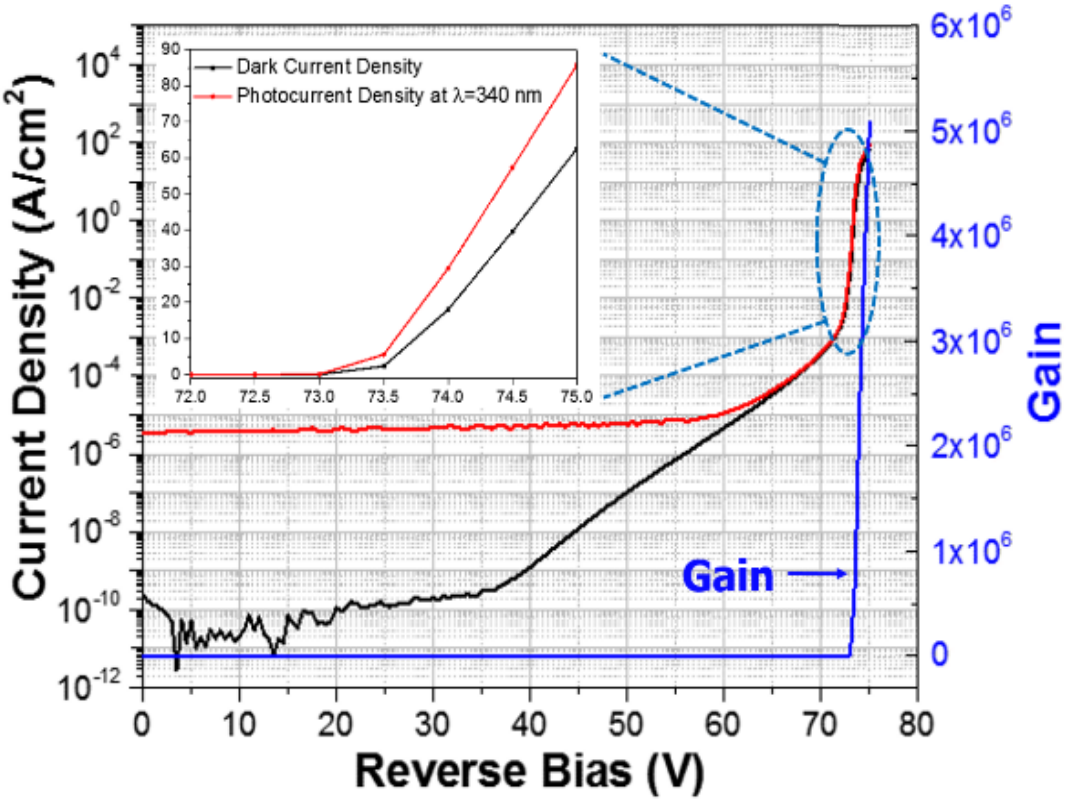

Figure 5: Reverse bias *I-V* and avalanche gain characteristics of GaN/AlGaN UV-APD with 75×75 μm^2 mesa size under dark conditions and UV illumination with peak wavelength of 340 nm.

The avalanche gain of the UV-APD plotted in Figure 5 is 7.8×10^3 at the onset point of voltage breakdown (~73 V). (This experimentally measured onset point is ~23 V lower than previously achieved with GaN/AlGaN *p-i-n* APDs and is in good agreement with simulated results [1,8].) At this point the gain is seen to rise exponentially corresponding to the sharp rise in photocurrent due to the avalanche multiplication process, reaching above 5×10^6 at a reverse bias of 75 V.

This sharp increase in the avalanche gain above the onset point of V_{BR} indicates that these fabricated UV-APD devices experience a strong avalanche multiplication process. As before, no microplasma breakdown or edge breakdown due to sidewall damage was observed, attributed to the low damage etching process and high-quality dielectric passivation utilized for the UV-APD devices. In addition, the increased maximum avalanche gain and reduced V_{BR} of the UV-APDs suggest that photogenerated electrons may be promoted to migrate toward the multiplication region by increasing the doping level of the charge layer through impact ionization.

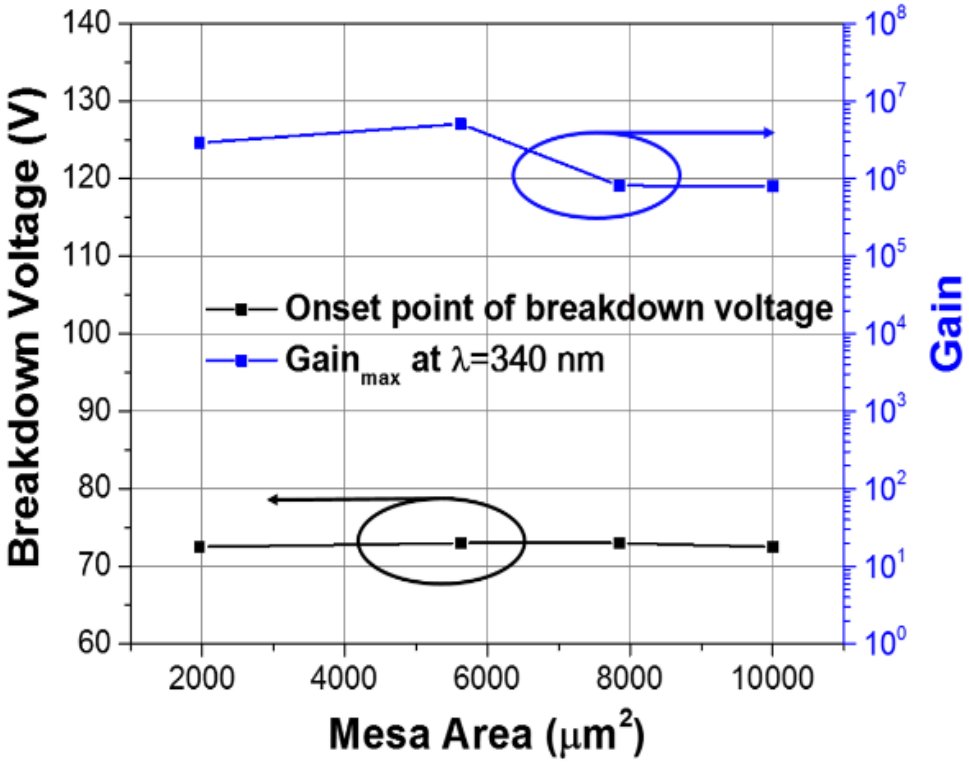

Figure 6: Reverse breakdown voltages and maximum avalanche gains of GaN/AlGaN UV-APD under 340 nm UV illumination plotted as functions of mesa area. The graph shows the area-dependent onset points of the breakdown voltages and maximum avalanche gains.

A comparison of the onset points of V_{BR} and the maximum gain properties of the UV-APDs for various mesa areas ranging from 1,963 μm^2 to 10,000 μm^2 is given in Figure 6. The onset points of V_{BR} of the UV-APDs with different mesa areas are seen to fall between 72.5 V and 73.0 V with small variation. These results are significantly better than that those previously measured for GaN/AlGaN UV-APDs having large detection areas, evidencing the high sensitivity of these GaN/AlGaN *p-i-p-i-n* UV-APDs compared to conventional *p-i-n* APDs [6]. This is attributed to homoepitaxial growth with reduced dislocation densities and defects, low etching damage, and application of high-quality passivation layers on the mesa sidewalls, which has enabled uniform onset points of V_{BR} in the UV-APDs with various large detection areas for NASA applications.

4.2 UV-APD spectral response

The bias-dependent spectral response of a GaN/AlGaN UV-APD with detector mesa size of 75×75 μm^2 was measured under frontside-illumination with an Oriel xenon lamp attached to a Cornerstone 260 monochromator/chopper system and lock-in amplifier. As shown in Figure 7, the zero-biased photocurrent exhibits a peak responsivity of 42.5 mA/W at 366 nm, corresponding to an EQE of 14% with an absorption edge at 390 nm.

It is noted that at a reverse bias of 70 V, the peak responsivity increases to 320 mA/W at 376 nm. In addition, with increasing reverse bias the peak absorption wavelength shifts slightly from 366 nm to 376 nm due to the Franz-Keldysh effect. Detection at the ~355 nm wavelength is achieved with higher concentrations of Al in AlGaN devices resulting in a blueshift of the absorption peak to this wavelength.

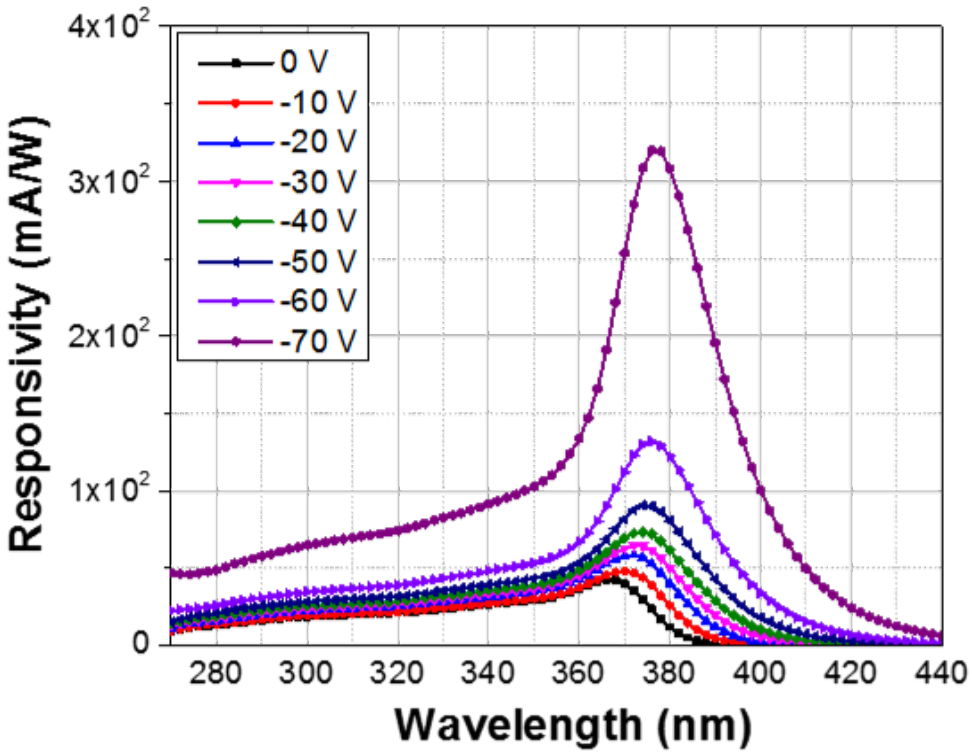

Figure 7: Reverse-voltage-dependent spectral response of GaN/AlGaN UV-APD with mesa size of 75×75 μm^2.

5. SUMMARY AND CONCLUSIONS

The high gain GaN AlGaN detectors and arrays developed by Georgia Tech and Magnolia on low defect density GaN substrates are advancing the state-of-the-art to provide enhanced capabilities for UV detection, particularly at the ~350 nm wavelength. GaN/AlGaN *p-i-p-i-n* separate UV-APDs with large detection areas have been demonstrated which exhibit high sensitivities compared to conventional *p-i-n* APDs. Superior gain properties and reductions in the breakdown voltage have been achieved through impact ionization engineering and made possible by the low dislocation substrates.

The development of GaN/AlGaN UV-APDs and APD arrays on GaN substrates with low dislocation densities for UV detection addresses technological issues associated with crystalline defects and crack formation in UV-APDs that have traditionally been detrimental to device performance and reliability. MOCVD epitaxial growth of AlGaN UV-APDs on native GaN substrates has enabled suppressed microplasma breakdown, providing low dark current densities with comparatively high photocurrents and responsivities over the UV spectrum. These improvements in GaN/AlGaN APD performance and reliability are key towards the development and successful implementation of robust, highly sensitive, high performance UV-APD detector arrays that will benefit future advanced NASA, defense, and commercial system applications.

ACKNOWLEDGEMENTS

This research is and has been funded by the National Aeronautics and Space Administration (NASA), Contract No. 80NSSC18C0093. The views and conclusions contained in this document are those of the authors and should not be interpreted as representing the official policies, either express or implied, of NASA or the U.S. Government.

REFERENCES

[1] Sood, A. K., Zeller, J. W., Welser, R. E., Puri, Y. R., Dupuis, R. D., Ji, M.-H., Kim, J., Detchprohm, T., Lewis, J., and Dhar, N. K., "Development of GaN/AlGaN UVAPDs for ultraviolet sensor applications," Int. J. Phys. Appl. 7(1), 49-58 (2015).

[2] Reine, M. B., Hairston, A., Lamarre, P., Wong, K. K., Tobin, S. P., Sood, A. K., Cooke, C., Pophristic, M., Guo, S., Peres, B., Singh, R., Eddy, Jr., C. R., Chowdhury, U., Wong, M. M., Dupuis, R. D., Li, T., and DenBaars, S. P., "Solar blind AlGaN 256x256 pin detectors and focal plane arrays," Proc. SPIE 6121, 61210R (2006).

[3] Sood, A. K., Richwine, R. A., Puri, Y. R., Dhar, N. K., Polla, D. L., and Wijewarnasuriya, P. S., "Multispectral EO/IR sensor model for evaluating UV, visible, SWIR, MWIR and LWIR system performance," Proc. SPIE 7300, 73000H (2009).

[4] Ji, M.-H., Kim, J., Detchprohm, T., Dupuis, R. D., Sood, A. K., Dhar, N. K., and Lewis, J., "Uniform and reliable GaN pin ultraviolet avalanche photodiode arrays," IEEE Photon. Tech. Lett. 28(19), 2015-2018 (2016).

[5] Zhou, Q., McIntosh, D. C., Lu, Z., Campbell, J. C., Sampath, A. V., Shen, H., and Wraback, M., "GaN/SiC avalanche photodiodes," Appl. Phys. Lett. 99, 131110 (2011).

[6] Kim, J., Ji, M.-H., Detchprohm, T., Ryou, J.-H, Dupuis, R. D., Sood, A. K., and Dhar, N. K., "$Al_xGa_{1-x}N$ ultraviolet avalanche photodiodes with avalanche gain greater than 10^5," IEEE Photon. Tech. Lett. 27(6), 642-645 (2015).

[7] Sood, A. K., Zeller, J. W., Puri, Y. R., Dupuis, R. D., Detchprohm, T., Ji, M.-H., Shen, S.-C., Babu, S., Dhar, N. K., and Wijewarnasuriya, P., "Development of high gain GaN/AlGaN avalanche photodiode arrays for UV detection and imaging applications," Int. J. Engr. Res. Tech. 10(2), 129-150 (2017).

[8] Ji, M.-H., Kim, J., Detchprohm, T., Dupuis, R. D., Sood, A. K., Dhar, N. K., and Lewis, J., "Uniform and reliable GaN pin ultraviolet avalanche photodiode arrays," IEEE Photon. Tech. Lett. 28(19), 2015-2018 (2016).